Angewandte Chemie

Polyoxometalates

Computer-Generated High-Valent Iron–Oxo and Manganese–Oxo Species with Polyoxometalate Ligands: How do they Compare with the Iron–Oxo Active Species of Heme Enzymes?**

Samuël P. de Visser, Devesh Kumar, Ronny Neumann, and Sason Shaik**

There is a continuing search for efficient and robust catalysts that can perform monooxygenation of organic compounds.[1] High-valent metal–oxo porphyrin species constitute such an important family.[2] The members of this family are analogous to the principal and potent oxidant of enzymes such as cytochrome P450 (CP450, **1**; Figure 1). Over the last two decades it has been gradually recognized that some transition-metal-substituted polyoxometalates (POMs) have intriguing properties as oxygenation catalysts.[3] These catalysts sometimes exhibit features that seem superficially similar to those observed with analogous metalloporphyrins. Thus, for example, it has been shown that Mn^{III}-substituted polyoxometalates, and to a much lesser extent also Fe^{III}-substituted compounds, catalyze oxygen-transfer reactions from iodosobenzene to alkenes and alkanes in a manner akin to the analogous metalloporphyrins.[4] The similarities between the transition-metal-substituted polyoxometalates and metalloporphyrin systems, and the postulate[4] that the active species of the transition-metal-substituted polyoxometalates catalysts may resemble the active species of CP450, endow the transition-metal-substituted polyoxometalates with added allure, and pose a problem worthy of theoretical interrogation.

The principal oxidant of CP450 is considered to be the triradicaloid Compound I species (**A**, Figure 1), which has two closely lying spin states with a quartet and doublet spin (^{4,2}**1**).[5] In both states, the iron atom in **A** is in oxidation state IV and the porphyrin (Por) is a radical cation, thus the entire complex can be briefly represented as $[(SH)Por^{\bullet+}\text{-}Fe^{IV}O]$. Therefore, the active species of CP450 and other

---

[*] Prof. R. Neumann
Department of Organic Chemistry
Weizmann Institute of Science
76100 Rehovot (Israel)
Fax: (+972) 8-9344142
E-mail: Ronny.Neumann@weizmann.ac.il

Dr. S. P. de Visser, Dr. D. Kumar, Prof. S. Shaik
Department of Organic Chemistry and The Lise Meitner-Minerva
Center for Computational Quantum Chemistry
Hebrew University, 91904 Jerusalem (Israel)
Fax: (+972) 2-6584680
E-mail: sason@yfaat.ch.huji.ac.il

[**] This research was supported by the Israel Science Foundation (S.S. and R.N.) and the Helen and Martin Kimmel Center for Molecular Design (R.N.). R.N. is the Rebecca and Israel Sieff Professor of Organic Chemistry.

Supporting information for this article is available on the WWW under http://www.angewandte.org or from the author.

DOI: 10.1002/ange.200453867
© 2004 Wiley-VCH Verlag GmbH & Co. KGaA, Weinheim

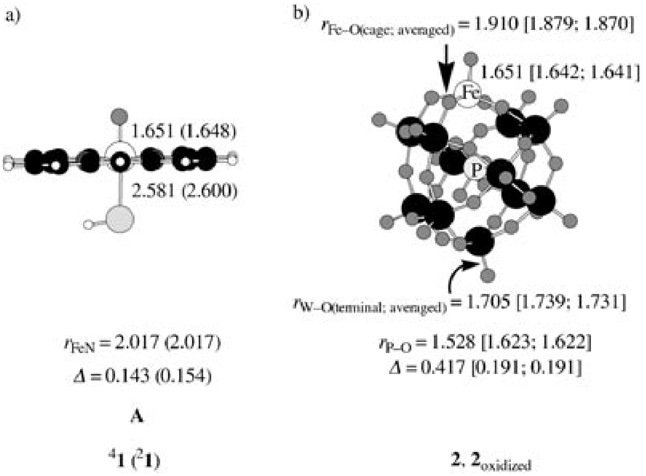

Figure 1. a) Optimized geometry of **A** (^{4,2}**1**) of CP450 in the quartet (doublet) spin states. b) The geometry generated from neutron diffraction data for the analogous $[POM\text{-}Fe{=}O]^{4-}$ (**2**) and $[POM\text{-}Fe{=}O]^{3-}$ ($\mathbf{2}_{oxidized}$) models, where POM is the $[PW_{11}O_{39}]^{7-}$ lacunary species or ligand. The values in square brackets are the respective optimized bond lengths for the high-spin states of the two species ^{4}**2** and $^{5}\mathbf{2}_{oxidized}$. All bond lengths are averaged values in Ångstroms; Δ is the displacement of the iron atom with respect to the four atoms of the plane of the porphyrin ring (in **1**) or to the four surface oxygen atoms on the sphere of the polyoxometalate.

heme enzymes has two oxidation equivalents above the resting state (the Fe^{III} complex), but only one equivalent resides on the iron center that appears in the Fe^{IV} oxidation state. Thus, the central questions to the study reported herein are: 1) How closely related to **A** are the corresponding POM–FeO species and 2) why, as might be expected from such an analogy, does the POM–Fe^{III} species not form a powerful catalyst, whereas the POM–Mn^{III} species which has one electron less does? To address these questions, we used density functional theory (DFT) to investigate the electronic structure of POM–FeO and POM–MnO complexes (POM is the $[PW_{11}O_{39}]^{7-}$ lacunary species or ligand). As shall be demonstrated, DFT predicts that the POM–FeO catalysts can sustain high oxidation states, as high as Fe^{V} and even the rare Fe^{VI} state, and also predicts that a highly electrophilic Mn^{VI}–oxo species could be generated for POM–MnO.

Earlier calculations[6] on polyoxometalate species of the Keggin structure, namely, $[PW_{12}O_{40}]^{3-}$, showed marginal differences between the neutron diffraction geometry and the DFT-optimized geometry. By using the same strategy, we started from $[PW_{12}O_{40}]^{3-}$ and generated $[PW_{11}O_{39}Fe{=}O]^{4-}$ (**2**) by the replacement of a single $\{W^{VI}{=}O\}^{4+}$ group by $\{Fe^{V}{=}O\}^{3+}$ and subsequently, using the same geometric parameters, we also calculated the one-electron-oxidized complex $[PW_{11}O_{39}Fe{=}O]^{3-}$ ($\mathbf{2}_{oxidized}$). For both complexes, we used the same Fe=O bond length as in **A**, namely 1.651 Å.[7] Subsequently, we optimized the structures (see the Supporting Information) for a few of the states of $[POM\text{-}Fe{=}O]^{4-}$ (**2**) and $[POM\text{-}Fe{=}O]^{3-}$ ($\mathbf{2}_{oxidized}$), and we ascertained that the optimum geometries did not differ markedly from those generated by the use of neutron-diffraction data on $[PW_{12}O_{40}]^{3-}$, at least with respect to the first coordination shell of the iron center. This finding can be seen from the key geometric details in Figure 1 b, which displays the neutron diffraction based data together with the optimized values in square brackets. Since each geometry optimization takes four months of CPU time, we restricted the rest of the study to the geometries generated from the neutron diffraction data. The $[POM\text{-}MnO]^{4-}$ (**3**) and $[POM\text{-}MnO]^{3-}$ ($\mathbf{3}_{oxidized}$) species were calculated with the same bond lengths as the iron analogues. All calculations were performed by using the Gaussian 98 program[8] with the hybrid B3LYP density functional method and the LANL2DZ basis set. The low-lying spin states of **2**, **3**, $\mathbf{2}_{oxidized}$, and $\mathbf{3}_{oxidized}$ were all examined. In addition, we verified the electronic structure of $[PW_{12}O_{40}]^{3-}$ (**4**), $[PW_{12}O_{40}]^{2-}$ ($\mathbf{4}_{oxidized}$),[6a] and of the resting-state species $[PW_{11}O_{39}FeOH_2]^{4-}$, as well as of the corresponding manganese complexes (see the Supporting Information). Here we focus on the transition-metal–oxo species.

Figure 2 shows the electronic structure of the POM–iron complex **2** with respect to **A** (^{2,4}**1**) of CP450 and illustrates the key orbitals of both species. The ground state of CP450 (on the left hand side) involves the well-known virtually degenerate set of doublet and quartet spin states with the common electronic configuration of $\delta^2\pi^*_{xz}{}^1\pi^*_{yz}{}^1a_{2u}{}^1$. With this occupation, the doublet and quartet spin states essentially correspond to a triplet Fe^{IV}–oxo moiety that is coupled ferro- and antiferromagnetically to a cation radical on the porphyrin ring, namely, $^{4,2}[(SH)Por^{\bullet+}Fe^{IV}O]$.

The right-hand side of Figure 2 shows the five d-block orbitals, labeled δ, π^*, and σ^* by analogy with the CP450 orbitals, that are virtually localized on the $\{(\text{-O-})_4Fe{=}O\}$ moiety of $[POM\text{-}FeO]^{4-}$. In addition, we show the highest occupied lone-pair orbital (lp_O), which is one of the many surface orbitals located on the bridging oxygen atoms and the oxo moieties of the W–O units of the polyoxometalate (see the Supporting Information). The ground state was found to be the high-spin quartet state ^{4}**2** with three singly occupied orbitals δ, π^*_{xz}, and π^*_{yz}. An analogous result was obtained by Siegbahn, Que, and co-workers[9] for the nonheme Fe^{V}–oxo species. The corresponding doublet state ^{2}**2**, with a β spin for the electron in the δ orbital, lies 12.8 kcal mol^{-1} (10.6 kcal mol^{-1} for the optimized geometries) higher in energy. This high energy of the antiferromagnetic state highlights the special stability of the high-spin half-filled π^*-δ shell, as a result of favorable exchange interactions. The importance of exchange stabilization is further made apparent by the $PorMn^{IV}$–oxo system[10] that was found previously to adopt the same half-filled configuration $\delta^1\pi^*_{xz}{}^1\pi^*_{yz}{}^1$.

Another doublet spin state with the occupancy $\delta^2\pi^*_{xz}{}^1\pi^*_{yz}{}^0$ was found to be 19.5 kcal mol^{-1} higher than the quartet state shown in Figure 2. An attempt to swap orbitals in ^{4}**2** and create an analogue of ^{4}**1** with the occupation $\delta^2\pi^*_{xz}{}^1\pi^*_{yz}{}^1lp_O{}^1$, akin to **A** (**1**), generated initially a high-energy species with a wave function that converged to the lower lying configuration $\delta^1\pi^*_{xz}{}^1\pi^*_{yz}{}^1$ in Figure 2. With three electrons in the δ, π^*_{xz}, and π^*_{yz} orbitals, all three ^{4,2}**2** states formally belong to the iron(v)–oxo situation.

In the gas-phase, the $[POM\text{-}Fe^{V}O]^{4-}$ species was computed to be unstable relative to its one-electron-oxidized form $[POM\text{-}FeO]^{3-}$, with an ionization potential (IP) of

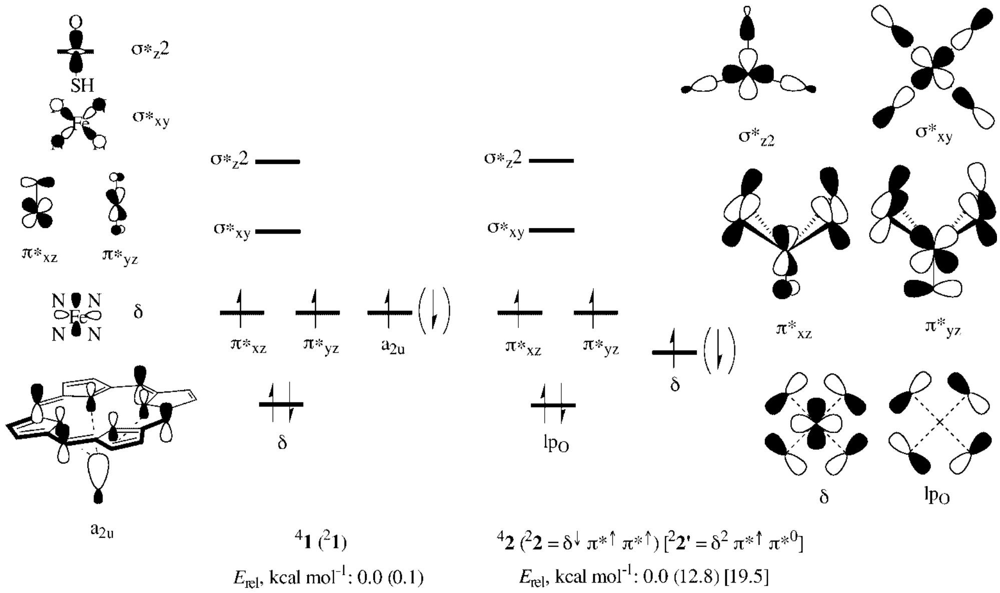

Figure 2. High-lying occupied and low-lying virtual orbitals of $^{4,2}\mathbf{1}$ (left-hand side) and the quartet and doublet states $^{4,2}\mathbf{2}$ (right-hand side) of $[\text{POM-FeO}]^{4-}$.

$-23.5\ \text{kcal mol}^{-1}$ (this is in contrast to the pristine unsubstituted POM for which the gas-phase IP is $65\ \text{kcal mol}^{-1}$). However, by using the continuum solvation model COSMO and a dielectric constant of water, the quadruply charged species was found to be stable and its ionization potential was calculated as $169.5\ \text{kcal mol}^{-1}$ (oxidation potential $= +2.8$ V, relative to the saturated hydrogen electrode (SHE)); a lower value would be expected for a less-polar solvent. The ground state of the one-electron-oxidized species is depicted in Figure 3a, and is seen to be the pair of quintet and triplet spin situations: $^{5,3}\mathbf{2}_{\text{oxidized}}$ with the $\delta^1\pi^*_{xz}{}^1\pi^*_{yz}{}^1\text{lp}_\text{O}{}^1$ electronic configuration. An excited state ($^1\mathbf{2}_{\text{oxidized}}$), with the $\delta^2\pi^*_{xz}{}^0\pi^*_{yz}{}^0\text{lp}_\text{O}{}^2$ electronic structure, lies $28.6\ \text{kcal mol}^{-1}$ higher in energy. Attempts to calculate the triplet states with either a $\delta^1\pi^*_{xz}{}^1\pi^*_{yz}{}^0$ or $\delta^0\pi^*_{xz}{}^1\pi^*_{yz}{}^1$ configuration resulted in convergence to the $\delta^1\pi^*_{xz}{}^1\pi^*_{yz}{}^1\text{lp}_\text{O}{}^1$ configuration. Thus, the generation of $^{5,3}\mathbf{2}_{\text{oxidized}}$ from $^{2,4}\mathbf{2}$ involves ejection of an electron from the surface orbitals of the POM and not from the d-type orbitals of the FeO moiety. This feature does not change when solvation is included.

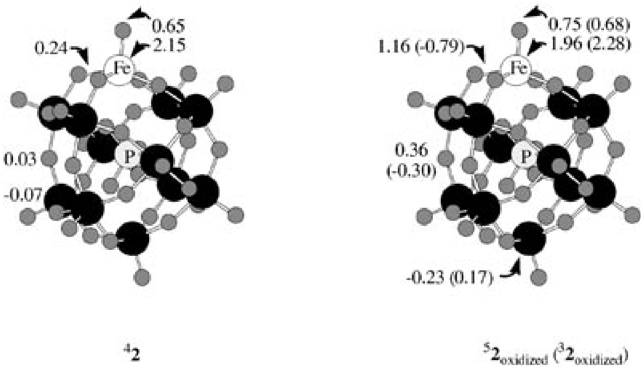

Figure 4. Spin-density distribution in the states of $^4\mathbf{2}$ and $^{5,3}\mathbf{2}_{\text{oxidized}}$ of $[\text{POM-FeO}]^{4-}$ and $[\text{POM-FeO}]^{3-}$.

Figure 4 shows the spin-density distribution in the lowest states of **2** and $\mathbf{2}_{\text{oxidized}}$ (for similar values in a solvent, see the Supporting Information). It is seen that, in accord with the electronic structure in Figure 2, most of the spin density (2.80) in $^4\mathbf{2}$ is localized on the FeO unit. Some spin density is located on the four oxygen ligands of FeO on the polyoxometalate surface (total spin: 0.24), while the rest of the cage atoms (W, O) together carry a small negative spin density (total: -0.04).

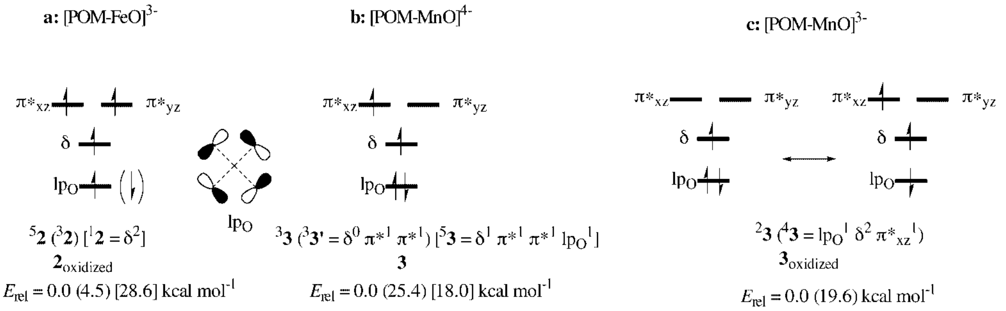

Figure 3. Electronic configurations and relative energies of a) the $^{5,3,1}\mathbf{2}_{\text{oxidized}}$ states of $[\text{POM-Fe}^{\text{VI}}\text{O}]^{3-}$; b) the $^{5,3}\mathbf{3}$ states of $[\text{POM-Mn}^{\text{V}}\text{O}]^{4-}$; and c) the $^{4,2}\mathbf{3}_{\text{oxidized}}$ states of $[\text{POM-Mn}^{\text{VI}}\text{O}]^{3-}$.

© 2004 Wiley-VCH Verlag GmbH & Co. KGaA, Weinheim

By contrast, the FeO unit in ${}^{5,3}\mathbf{2}_{\text{oxidized}}$ carries three spins, while the fourth is on the polyoxometalate surface, and mostly near the coordination sphere of the FeO unit, again in accord with the electronic structure in Figure 3. Clearly, whereas the $[\text{POM-Fe}^{\text{V}}{=}\text{O}]^{4-}$ complex (**2**) does not resemble the isoelectronic **A** species, the one-electron-oxidized species, which is effectively Fe^{VI}, resembles **A** and can be written briefly as $[\text{POM}^{\bullet+}\text{Fe}^{\text{V}}{=}\text{O}]^{3-}$, with a quartet Fe=O unit coupled ferro- and antiferromagnetically to the $\text{POM}^{\bullet+}$ unit, which is in accord with the $\delta^1\pi^{*}{}_{xz}{}^{1}\pi^{*}{}_{yz}{}^{1}\text{lp}_{\text{O}}{}^{1}$ occupancy discussed above.

A few major factors are responsible for these electronic differences and similarities between the polyoxometalate and the CP450 species. The first one is clearly the different geometry of the two compounds. As can be seen in Figure 1, the porphyrin is planar and the iron atom in CP450 lies close to the plane of the ring ($\Delta = 0.14, 0.15$ Å). In comparison, the iron atom in the polyoxometalate lies higher above the plane of the four coordinated oxygen atoms at a distance of 0.42 Å (0.191 Å in the optimum structure). As seen in Figure 2, this endows the d-type $\pi^{*}{}_{xz}$ and $\pi^{*}{}_{yz}$ orbitals of the FeO moiety of POM–FeO with antibonding interactions from the four POM oxygen atoms in the coordination sphere of the iron center. This effect raises the energy of the π* orbitals and stabilizes the oxidation state of iron(v) in ${}^{4}\mathbf{2}$ relative to that of the porphyrin moiety in which the π* orbitals are low lying and the Fe^{V} state is less stable than the $[\text{Por}^{\bullet+}\text{Fe}^{\text{IV}}]$ situation.[7] This effect is similar to that discussed for the pentacoordinate metallocorrole complexes,[11] and to the findings in non-heme iron complexes.[9] Another effect concerns the δ orbital in Figure 2. Thus, unlike the metalloporphyrin system, where this orbital is a very low-lying purely nonbonding orbital with preferred double occupancy, this orbital in the POM–FeO complexes is high-lying because of the antibonding interaction with the four polyoxometalate oxygen atoms in the first coordination sphere. Consequently, the π* and δ orbitals of POM–FeO become almost degenerate, and prefer the high-spin and exchange-stabilized $\delta^1\pi^{*}{}_{xz}{}^{1}\pi^{*}{}_{yz}{}^{1}$ subshell in all its complexes. This situation generates, in turn, the ferro- and antiferromagnetic pair of states ${}^{5,3}\mathbf{2}_{\text{oxidized}}$, which retain the half-filled δ-π* subshell and have an additional unpaired electron on the polyoxometalate surface. Consequently, these complexes can be represented as ${}^{5,3}[\text{POM}^{\bullet+}\text{Fe}^{\text{V}}{=}\text{O}]^{3-}$, and are, therefore, the polyoxometalate analogues of ${}^{4,2}\mathbf{A}$ in the heme system, but with an Fe^{V} center instead of Fe^{IV}.

Our calculations (see Figure 3b) further show that $[\text{POM-MnO}]^{4-}$ has a triplet ground state that differs from the isoelectronic iron species $[\text{POM}^{\bullet+}\text{Fe}^{\text{V}}{=}\text{O}]^{3-}$. Thus, while the iron species has a half-filled δ-π* subshell coupled to an unpaired electron on the polyoxometalate surface (Figure 3a), the manganese species is a triplet state with a $\delta^1\pi^{*1}$ configuration; the other manganese states are significantly higher in energy. Thus, in fact, the ground state of the manganese complex corresponds to $[\text{POM-Mn}^{\text{V}}{=}\text{O}]^{4-}$, with Mn being in oxidation state v. Once again, in the gas phase, the quadruply charged complex is unstable towards the loss of one electron and leads to $[\text{POM-Mn}{=}\text{O}]^{3-}$ ($\mathbf{3}_{\text{oxidized}}$, Figure 3c). In solution, however, the ionization potential is substantial and positive (171.5 kcal mol^{-1}). The resulting $\mathbf{3}_{\text{oxidized}}$ complex has a doublet ground state (${}^{2}\mathbf{3}_{\text{oxidized}}$) that is well-separated from its quartet-spin excited state (${}^{4}\mathbf{3}_{\text{oxidized}}$). Its electronic structure and spin distribution (see the Supporting Information) fits best to a mixed configuration between $\delta^1\pi^{*}{}_{xz}{}^{0}\pi^{*}{}_{yz}{}^{0}\text{lp}_{\text{O}}{}^{2}$ and $\delta^1\pi^{*}{}_{xz}{}^{1}\pi^{*}{}_{yz}{}^{0}\text{lp}_{\text{O}}{}^{1}$, and thereby corresponds to the mixed-valent species $[\text{POM-Mn}^{\text{VI}}{=}\text{O}]^{3-} \leftrightarrow [\text{POM}^{\bullet+}\text{Mn}^{\text{V}}\text{O}]^{3-}$.

Finally, our calculations on the water complexes $[\text{PW}_{11}\text{O}_{39}\text{FeOH}_2]^{4-}$ (**5**) and $[\text{PW}_{11}\text{O}_{39}\text{MnOH}_2]^{4-}$ (**6**) show that these are iron(iii)-aqua and manganese(iii)-aqua complexes, with frontier orbitals localized on the MOH_2 moiety (M = Fe, Mn; see Supporting Information). As such, it is conceivable that these complexes can be converted into iron–oxo and manganese–oxo complexes by the usual techniques, for example, using iodosobenzene.[2c] The identity of the species that carries out the catalytic oxidation is not really known,[4] and it is therefore essential to consider both the quadruply and triply charged forms of the iron and manganese complexes. Comparison of **2** with **3** shows that the iron reagent $[\text{POM-Fe}^{\text{V}}{=}\text{O}]^{4-}$ (${}^{2,4}\mathbf{2}$) has a half-filled δ-π* subshell, whereas the manganese reagent $[\text{POM-Mn}^{\text{V}}{=}\text{O}]^{4-}$ (${}^{3}\mathbf{3}$) has a vacant π* orbital. Similarly, in the oxidized form, the ${}^{5}\mathbf{2}_{\text{oxidized}}$ ground state of $[\text{POM}^{\bullet+}\text{Fe}^{\text{V}}\text{O}]^{3-}$ has a half-filled δ-π* subshell, while the ${}^{2}\mathbf{3}_{\text{oxidized}}$ ground state of $[\text{POM}^{\bullet+}\text{Mn}^{\text{VI}}\text{O}]^{3-}$ has largely vacant π* orbitals. Thus, by analogy with other electrophiles we expect that both $[\text{POM-Mn}^{\text{V}}{=}\text{O}]^{4-}$ and $[\text{POM}^{\bullet+}\text{Mn}^{\text{VI}}\text{O}]^{3-}$ will be highly electrophilic species as a consequence of the vacant π* orbitals, while both $[\text{POM-Fe}^{\text{V}}{=}\text{O}]^{4-}$ and $[\text{POM}^{\bullet+}\text{Fe}^{\text{V}}\text{O}]^{3-}$, with the half-filled subshell, will be sluggish and less-stereoselective oxidants like $[\text{PorMn}^{\text{IV}}\text{O}]$.[12] These expectations appear to be in accord with experimental data[4] on the oxidative capabilities of the two transition-metal-substituted polyoxometalate systems.

Our study shows that the polyoxometalate system affords a convenient platform for the generation of metal–oxo species with high oxidation states of the transition metal, as much as v and vi. The intriguing analogy of the POM–FeO and POM–MnO species to the **A** species of P450 appears to get reasonable theoretical support. However, the oxidation state of the metal in the POM complexes is, respectively, one and two units higher than **A**. Furthermore, the electronic structure proposed herein is sufficiently interesting to attempt its identification by experimental means.

Received: January 27, 2004 [Z53867]

Keywords: cytochrome P450 · density functional calculations · metalloporphyrins · oxidation · polyoxometalates

---

[1] *Biomimetic Oxidations Catalyzed by Transition Metal Complexes* (Ed.: B. Meunier), Imperial College Press, London, **1999**.

[2] a) B. Meunier, J. Bernadou, *Struct. Bonding (Berlin)* **2000**, *97*, 1–35; b) Y. Watanabe in *The Porphyrin Handbook*, *Vol. 4* (Eds.: K. M. Kadish, K. M. Smith, R. Guilard), Academic Press, San Diego, **2000**, pp. 97–117; c) J. T. Groves, K. Shalyaev, J. Lee in *The Porphyrin Handbook*, *Vol. 4* (Eds.: K. M. Kadish, K. M. Smith, R. Guilard), Academic Press, San Diego, **2000**, pp. 17–40.

[3] a) I. V. Kozhevnikov, *Chem. Rev.* **1998**, *98*, 171–198; b) N. Mizuno, M. Misono, *Chem. Rev.* **1998**, *98*, 199–217; c) R.

Neumann, *Prog. Inorg. Chem.* **1998**, *47*, 317–370; d) C. L. Hill, C. M. Prosser-McCartha, *Coord. Chem. Rev.* **1995**, *43*, 407–455.

[4] a) C. L. Hill, R. B. Brown, Jr., *J. Am. Chem. Soc.* **1986**, *108*, 536–538; b) D. Mansuy, J.-F. Bartoli, P. Battioni, D. K. Lyon, R. G. Finke, *J. Am. Chem. Soc.* **1991**, *113*, 7222–7226.

[5] D. L. Harris, *Curr. Opin. Chem. Biol.* **2001**, *5*, 724–735.

[6] a) J. M. Maestre, X. López, C. Bo, J.-M. Poblet, N. Casañ-Pastor, *J. Am. Chem. Soc.* **2001**, *123*, 3749–3758; b) S. Ganapathy, M. Fournier, J. F. Paul, L. Delevoye, M. Guelton, J. P. Amoureux, *J. Am. Chem. Soc.* **2002**, *124*, 7821–7828; c) N. Suaud, A. Gaita-Ariño, J. M. Clemente-Juan, J. Sánchez-Marín, E. Coronado, *J. Am. Chem. Soc.* **2002**, *124*, 15134–15140; d) J. M. Poblet, X. López, C. Bo, *Chem. Soc. Rev.* **2003**, *32*, 297–308; e) see, however, A. J. Bridgeman, *Chem. Eur. J.* **2004**, *10*, 2935–2941.

[7] F. Ogliaro, S. P. de Visser, J. T. Groves, S. Shaik, *Angew. Chem. Int. Ed.* **2001**, *40*, 2874–2878.

[8] Gaussian 98 (Revision A.7), M. J. Frisch, G. W. Trucks, H. B. Schlegel, G. E. Scuseria, M. A. Robb, J. R. Cheeseman, V. G. Zakrzewski, J. A. Montgomery, R. E. Stratmann, J. C. Burant, S. Dapprich, J. M. Millam, A. D. Daniels, K. N. Kudin, M. C. Strain, O. Farkas, J. Tomasi, V. Barone, M. Cossi, R. Cammi, B. Mennucci, C. Pomelli, C. Adamo, S. Clifford, J. Ochterski, G. A. Petersson, P. Y. Ayala, Q. Cui, K. Morokuma, D. K. Malick, A. D. Rabuck, K. Raghavachari, J. B. Foresman, J. Cioslowski, J. V. Ortiz, B. B. Stefanov, G. Liu, A. Liashenko, P. Piskorz, I. Komaromi, R. Gomperts, R. L. Martin, D. J. Fox, T. Keith, M. A. Al-Laham, C. Y. Peng, A. Nanayakkara, C. Gonzalez, M. Challacombe, P. M. W. Gill, B. G. Johnson, W. Chen, M. W. Wong, J. L. Andres, M. Head-Gordon, E. S. Replogle, J. A. Pople, Gaussian, Inc., Pittsburgh, PA, **1998**.

[9] A. Bassan, M. R. A. Blomberg, P. E. M. Siegbahn, L. Que, Jr, *J. Am. Chem. Soc.* **2002**, *124*, 11056–11063.

[10] a) R. S. Czernuszewicz, Y. O. Su, M. K. Stern, K. A. Macor, D. Kim, J. T. Groves, T. G. Spiro, *J. Am. Chem. Soc.* **1988**, *110*, 4158–4165; b) J. T. Groves, J. Lee, S. S. Marla, *J. Am. Chem. Soc.* **1997**, *119*, 6269–6273; c) see, however, [PorMn^{V}O] in: N. Jin, J. T. Groves, *J. Am. Chem. Soc.* **1999**, *121*, 2923–2924.

[11] S. P. de Visser, F. Ogliaro, Z. Gross, S. Shaik, *Chem. Eur. J.* **2001**, *7*, 4954–4960.

[12] J. T. Groves, M. K. Stern, *J. Am. Chem. Soc.* **1987**, *109*, 3812–3814.

© 2004 Wiley-VCH Verlag GmbH & Co. KGaA, Weinheim